HYPERSPECTRAL IMAGE ANALYSIS WITH PIECE-WISE CONVEX ENDMEMBER ESTIMATION AND SPECTRAL UNMIXING

Alina Zare[1], Ouiem Bchir[2], Hichem Frigui[3], and Paul Gader[4]

[1]Electrical and Computer Engineering, University of Missouri, Columbia, MO 65211
[2]Computer Science, King Saud University, Riyadh, Saudi Arabia
[3]Computer Science & Computer Engineering, University of Louisville, Louisville, KY 40292
[4]Computer & Information Science & Engineering, University of Florida, Gainesville, FL 32611

ABSTRACT

A hyperspectral endmember detection and spectral unmixing algorithm that finds multiple sets of endmembers is presented. This algorithm, the Piece-wise Convex Multiple Model Endmember Detection (P-COMMEND) algorithm, models a hyperspectral image using a piece-wise convex representation. By using a piece-wise convex representation, non-convex hyperspectral data are more accurately characterized. For example, the well-known Indian Pines hyperspectral image is used as an example of a piece-wise convex collection of pixels. The convex regions, weights, endmembers and abundances are found using an iterative fuzzy clustering method. Results indicate that the piece-wise convex representation provides endmembers that better represent hyperspectral data sets over methods that use a single convex region.

Index Terms— hyperspectral, unmixing, endmember.

1. INTRODUCTION

The spectral signatures of the pure materials in a hyperspectral scene are often referred to as *endmembers* [1]. *Spectral unmixing* is the task of decomposing pixels from a hyperspectral image into their respective endmembers and *abundances*. Abundances are the proportions of every endmember in each pixel in a hyperspectral image. The standard model used to perform spectral unmixing is the *convex geometry model* (also known as the *linear mixing model*). This model states that every pixel is a convex combination of endmembers in the scene. This has been shown in the literature to hold in cases where the spectra of the endmember are mixed by the spatial resolution of the imaging sensor [1, 2]. If the convex geometry model holds, the endmembers are the spectra found at the corners of a convex region enclosing all the spectra in a hyperspectral scene. This model can be written as $\mathbf{x}_i = \sum_{k=1}^{M} p_{ik}\mathbf{e}_k + \epsilon_i \quad i = 1, \ldots, N$ where N is the number of pixels in the image, M is the number of endmembers, ϵ_i is an error term, p_{ik} is the proportion of endmember k in pixel i, and $\mathbf{e}_k$ is the k^{th} endmember. The proportions of this model satisfy the constraints: $p_{ik} \geq 0 \quad \forall k = 1, \ldots, M; \quad \sum_{k=1}^{M} p_{ik} = 1$.

In the algorithm presented here, the **P**iece-wise **Co**nvex **M**ultiple **M**odel **End**member Detection (P-COMMEND) algorithm, several sets of endmembers are found to describe hyperspectral image data. Each endmember set is found using the convex geometry model resulting in a piece-wise convex representation of the hyperspectral data.

Consider the AVIRIS Indian Pines [3] hyperspectral data set. When applying principal components analysis (PCA) and reducing dimensionality down to three dimensions, the resulting data set appears piece-wise convex, as shown in Figure 1. This real hyperspectral data is not convex. Instead, a piece-wise convex representation would provide a better fit.

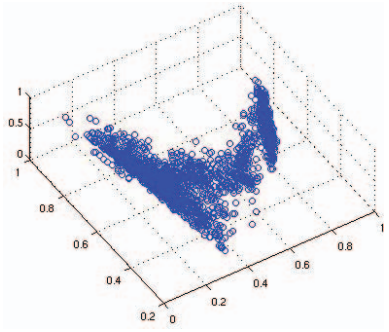

Fig. 1. The AVIRIS Indian Pines hyperspectral data set after applying PCA for dimensionality reduction to 3 dimensions.

The piece-wise convex representation for hyperspectral imagery was first used by Zare in [4] as well as by Zare and Gader in [5] and [6]. These methods sample from a Dirichlet Process to partition the input hyperspectral data into convex regions. In contrast, the P-COMMEND algorithm applies a novel fuzzy clustering approach to the piece-wise convex representation for hyperspectral endmember detection and spectral unmixing. Therefore, the previous Dirichlet process approach finds crisp partitions and autonomously determines the number of convex regions needed where the proposed method

determines fuzzy clusters of the data. Many endmember detection and spectral unmixing algorithms have been proposed in the literature. A number of these methods rely on the pixel purity assumption and assume the endmembers can be found within the data set [7]. Methods have also been developed based on Non-Negative Matrix Factorization [8], Independent Components Analysis [9] and others. However, all of these methods search for a single set of endmembers and, therefore, a single convex region to describe a hyperspectral scene. Since these algorithms assume a single convex region, they cannot find appropriate endmembers for non-convex data.

2. PIECE-WISE CONVEX MULTIPLE MODEL ENDMEMBER DETECTION

The objective function for the proposed method is shown in Equation 1.

$$\begin{aligned} J &= \sum_{i=1}^{C}\sum_{j=1}^{N} u_{ij}^{m} \left(\mathbf{x}_j - \mathbf{E}_i\mathbf{p}_{ij}\right)^T \left(\mathbf{x}_j - \mathbf{E}_i\mathbf{p}_{ij}\right) \\ &+ \alpha\sum_{i=1}^{C}\left(M \cdot trace(\mathbf{E}_i^T\mathbf{E}_i) - 1_{1\times M}\mathbf{E}_i^T\mathbf{E}_i 1_{M\times 1}\right) \end{aligned}$$

The objective function described by Equation (1) is minimized with respect to $\mathbf{E}_i$, $\mathbf{p}_{ij}$ and u_{ij} while enforcing non-negativity and sum-to-one constraints on the proportions and membership values. The resulting update equations are shown below.

The update equation for the endmembers are:

$$\mathbf{E}_i = \left(\sum_j u_{ij}^m \mathbf{p}_{ij}\mathbf{p}_{ij}^T + 2\alpha D\right)^{-1}\left(\sum_j u_{ij}^m \mathbf{p}_{ij}\mathbf{x}_j^T\right) \quad (1)$$

where

$$D = M\mathbf{I}_{M\times M} - \mathbf{1}_{M\times M} \quad (2)$$

Minimization of the objection function with respect to $\mathbf{p}_{ij}$ results in the following.

$$\mathbf{p}_{ij} = \left(\mathbf{E}_i^T\mathbf{E}_i\right)^{-1}\left(\mathbf{E}_i^T\mathbf{x}_j - \frac{\lambda_i}{2}1_{M\times 1}\right) \quad (3)$$

where

$$\lambda_i = 2\frac{1_{1\times M}\left(\mathbf{E}_i^T\mathbf{E}_i\right)^{-1}\mathbf{E}_i^T\mathbf{x}_j - 1}{1_{1\times M}\left(\mathbf{E}_i^T\mathbf{E}_i\right)^{-1}1_{M\times 1}} \quad (4)$$

KKT conditions [10] are enforced resulting in clipping negative proportion values to zero.

$$\mathbf{p}_{ij}^{KKT} = max\left(\mathbf{p}_{ij}, 0\right) \quad (5)$$

Finally, the update equation for the membership values are as shown in the following equation.

$$u_{ij} = \frac{\left(\frac{1}{(m-1)(\mathbf{x}_j-\mathbf{E}_i\mathbf{p}_{ij})^T(\mathbf{x}_j-\mathbf{E}_i\mathbf{p}_{ij})}\right)^{\frac{1}{m-1}}}{\sum_{q=1}^{C}\left(\frac{1}{(\mathbf{x}_j-\mathbf{E}_q\mathbf{p}_{qj})^T(\mathbf{x}_j-\mathbf{E}_q)\mathbf{p}_{qj}}\right)^{\frac{1}{m-1}}} \quad (6)$$

Algorithm 1 The P-COMMEND algorithm

Fix number of clusters C and m $\in [1,\infty)$, α, M;
Initialize the fuzzy partition matrix U;
Initialize the set of abundance matrices $\{\mathbf{p}_{ij}\}_{i=1,\ldots,C;j=1,\ldots,N}$.

REPEAT

Update endmembers matrices $\{\mathbf{E}_i\}_{i=1,\ldots,C}$ using (1);

Update the set of abundances $\{\mathbf{p}_{ij}\}_{i=1,\ldots,C;j=1,\ldots,N}$ using (3) and (4);

Apply the KKT condition on $\{\mathbf{p}_{ij}\}_{i=1,\ldots,C;j=1,\ldots,N}$ using (5) and renormalize;

Update the fuzzy membership using (6);

UNTIL convergence critera are met

Currently, the endmembers are randomly initialized to randomly selected input hyperspectral pixels. The proportion values are randomly initialized by drawing from a uniform Dirichlet distribution. Membership values are initialized using the fuzzy c-means algorithm (which is, in turn, randomly initialized). Furthermore, convergence is checked by comparing the difference between the $\mathbf{E}$, $\mathbf{P}$, and $\mathbf{U}$ from successive iterations until change falls below a prescribed threshold.

3. EXPERIMENTAL RESULTS

In the following, P-COMMEND is tested using the June 1992 AVIRIS Indian Pines data set [3]. These data were collected over the Indian Pines test site in an agricultural area of northern Indiana. The image has 145×145 pixels with 220 spectral bands. The data contains approximately two-thirds agricultural land and one-third forest and other elements [11]. Figure 2 shows an image of band 10 (approximately 0.49 μm) and the ground truth for this data set. Results were compared to the ICE [12] and VCA [7] endmember estimation methods. The Maximum Noise Fraction (MNF) algorithm [13] was used to reduce the dimensionality of the data to nine dimensions prior to running the endmember detection algorithms.

In order to compare P-COMMEND and ICE on this data set, the parameter settings were set such that the residual errors resulting from the two methods are similar. Specifically, the parameters were set to $M = 3$, $C = 2$, $\alpha = 1$ and $m = 1.3$ for P-COMMEND and $\mu = 0.0125$ for ICE. These resulted in total squared residual error values of 1.29 and 1.25 for P-COMMEND and ICE, respectively. Given that the residual errors are comparable, then the distribution of abundance values across the endmembers for each class in the Indian Pines data set is considered. The abundance values found by P-COMMEND for each class are concentrated to a smaller number of endmembers than the abundance val-

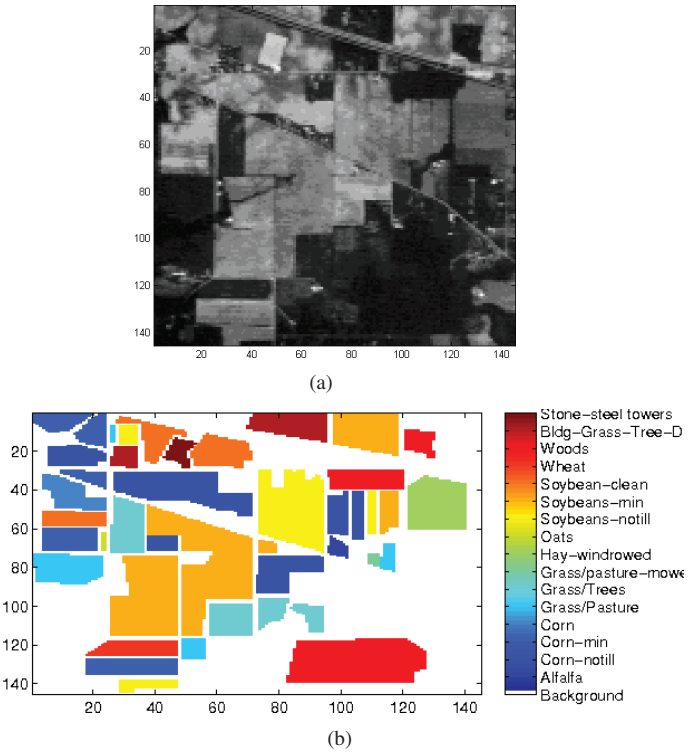

Fig. 2. (a) Band 10 (0.49 μm) of the AVIRIS Indian Pines data set (b) The ground truth of the AVIRIS Indian Pines data set.

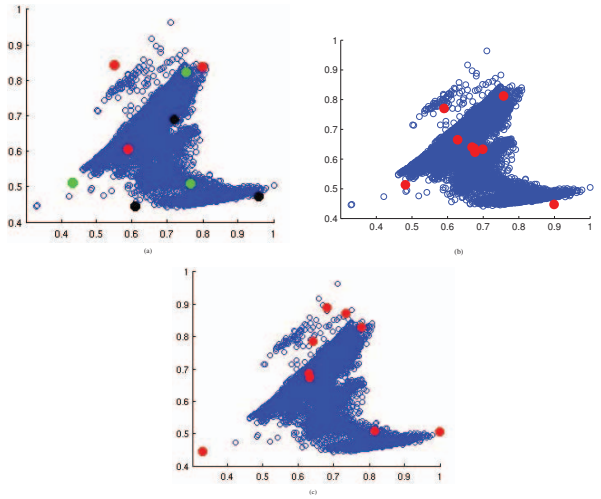

Fig. 3. A scatterplot of the first two MNF bands of the AVIRIS Indian Pines data set and the endmembers results using (a) P-COMMEND (b) ICE and (c) VCA. The various colors of the endmembers in the P-COMMEND result correspond to the different partitions. Endmembers of the same color are in the same convex region.

ues found by ICE. For each class, Shannon's entropy of the normalized distribution of abundance values was computed [14]. A smaller entropy value indicates that the abundances associated with a single class are concentrated onto a smaller number of endmembers. Table 1 lists the entropy values computed for each class using the abundances found by P-COMMEND, ICE and VCA. The P-COMMEND results are generally smaller indicating that the abundances for each class are concentrated onto a smaller number of endmembers and, therefore, the endmembers provide a better representation of the input data. In fact, entropy can be thought of as a measure of pixel purity since an entropy of 0 would indicate a pure pixel (identical to the endmember) and a maximum entropy from abundances of $\frac{1}{M}$ would indicate a highly mixed pixel. A scatter plot of the first MNF bands found using the ICE and P-COMMEND algorithms are shown in Figure 3. As seen in the figure, the ICE algorithm surrounds the data with four endmembers and places the remaining endmembers near the mean of the data. In contrast, the P-COMMEND algorithm separates out the convex regions in the data.

4. DISCUSSION AND FUTURE WORK

The P-COMMEND algorithm provides an endmember detection and spectral unmixing method that utilizes a piece-wise convex representation of hyperspectral imagery. The piece-wise convex representation allows several sets of endmembers to be determined. For each set of endmembers, the convex geometry model is applied and spectral unmixing is performed. As the results indicate, the piece-wise convex representation of hyperspectral imagery provides a better representation of the input data sets when compared to a single convex region.

Future work for this method include autonomously estimating the number of endmembers and the number of convex regions. Currently, we assume that the number of convex regions and the number of endmembers per cluster are known apriori. Moreover, we plan to investigate an automatic determination of the number of the balancing parameter α.

5. REFERENCES

[1] N. Keshava and J. F. Mustard, "Spectral unmixing," *IEEE Signal Processing Magazine*, vol. 19, pp. 44–57, 2002.

[2] D. Manolakis, D. Marden, and G. A. Shaw, "Hyperspectral image processing for automatic target detection applications," *Lincoln Laboratory Journal*, vol. 14, no. 1, pp. 79–116, 2003.

[3] AVIRIS, ," (2004, Sep) AVIRIS free standard data products. Jet Propulsion Laboratory, California Institute of Technology, Pasedena, CA. URL http://aviris.jpl.nasa.gov/html/aviris.freedata.html.

Table 1. Comparison of the Shannon entropy values for the distribution of abundance values across endmembers associated with each ground truth label.

	P-COMMEND Entropies	ICE Entropies	VCA Entropies
Alfalfa	1.3	1.5	1.7
Corn-no till	1.6	1.8	1.8
Corn-min	1.6	1.9	1.9
Corn	1.4	1.8	1.9
Grass/Pasture	1.4	1.3	1.8
Grass/Trees	1.1	1.4	1.6
Grass/Pasture-Mowed	1.4	1.8	1.8
Hay-windrowed	0.8	1.4	1.7
Oats	1.3	1.6	1.9
Soybeans-notill	1.7	1.9	1.7
Soybeans-min	1.6	1.9	1.7
Soybeans-clean	1.6	1.9	1.9
Wheat	0.9	1.0	1.6
Woods	0.8	0.8	1.3
Bldg-Grass-Trees-Drives	1.6	1.3	1.8
Stone-steel Towers	1.0	0.7	1.7

[4] A. Zare, *Hyperspectral Endmember Detection and Band Selection using Bayesian Methods*, Ph.D. thesis, University of Florida, 2009.

[5] A. Zare and P. Gader, "PCE: Piece-wise convex endmember detection," *IEEE Transactions on Geoscience and Remote Sensing*, vol. 48, no. 6, pp. 2620–2632, Jun. 2010.

[6] A. Zare and P. Gader, "Context-based endmember detection for hyperspectral imagery," in *Proceedings of the First IEEE Workshop on Hyperspectral Image and Signal Processing: Evolution in Remote Sensing*, Grenoble, France, Aug. 2009.

[7] J. M. P. Nascimento and J. M. Bioucas-Dias, "Vertex component analysis: A fast algorithm to unmix hyperspectral data," *IEEE Transactions on Geoscience and Remote Sensing*, vol. 43, no. 4, pp. 898–910, Apr. 2005.

[8] S. Jia and Y Qian, "Constrained nonnegative matrix factorization for hyperspectral unmixing," *IEEE Transactions on Geoscience and Remote Sensing*, vol. 47, no. 1, pp. 161–173, Jan. 2009.

[9] J. Wang and C.-I. Chang, "Applications of independent component analysis in endmember extraction and abundance quantification for hyperspectral imagery," *IEEE Transactions on Geoscience and Remote Sensing*, vol. 44, no. 9, pp. 2601–2616, Sept. 2006.

[10] H. W. Kuhn and A. W. Tucker, *Nonlinear programming*, Proceedings of 2nd Berkeley Symposium, 1951.

[11] S. B. Serpico and L. Bruzzone, "A new search algorithm for feature selection in hyperspectral remote sensing images," *IEEE Transactions on Geoscience and Remote Sensing*, vol. 39, no. 7, pp. 1360–1367, July 2001.

[12] M. Berman, H. Kiiveri, R. Lagerstrom, A. Ernst, R. Dunne, and J. F. Huntington, "ICE: A statistical approach to identifying endmembers in hyperspectral images," *IEEE Transactions on Geoscience and Remote Sensing*, vol. 42, pp. 2085–2095, Oct. 2004.

[13] A. A. Green, M. Berman, P. Switzer, and M. D. Craig, "A transformation for ordering multispectral data in terms of image quality with implications for noise removal," *IEEE Transactions on Geoscience and Remote Sensing*, vol. 26, pp. 65–73, Jan. 1988.

[14] D. J. C. MacKay, *Information Theory, Inference & Learning Algorithms*, Cambridge University Press, 2002.